



Effect of heat treatment on adsorption performance and photocatalytic activity of TiO₂-mounted activated carbon cloths

Deping Xu^{a,b}, Zheng-Hong Huang^{a,*}, Feiyu Kang^a, M. Inagaki^c, T.-H. Ko^d

^a Lab of Advanced Materials, Department of Materials Science and Engineering, Tsinghua University, Beijing 100084, China

^b School of Chemical and Environmental Engineering, China University of Mining and Technology, Beijing 100083, China

^c Department of Applied Chemistry, Aichi Institute of Technology, Toyota 470-0392, Japan

^d Department of Materials Science, Feng Chia University, Taichung, Taiwan, China

ARTICLE INFO

Article history:

Available online 10 September 2008

Keywords:

Porous carbon
Catalyst support
Reactivity

ABSTRACT

Photoactive TiO₂ was homogeneously mounted on PAN-based activated carbon cloths (ACCs) by a process of dip-coating and subsequent annealing in nitrogen atmosphere. The crystallinity of TiO₂ and pore structure of hybrids was characterized by XRD and N₂ adsorption. The adsorption and photocatalytic activity for TiO₂-mounted ACC towards methylene blue (MB) solution was investigated. The results showed that the coating of TiO₂ gel resulted in a marked decrease in specific surface area and pore volume from the pristine ACC, which was recovered gradually with increasing treatment temperature. Besides crystallinity of TiO₂ can be modified by heat treatment, its pore structure can be postulated by adding different amount of polyethylene glycol (PEG). Both pore structure of hybrids and crystallinity of TiO₂ as well as the carbon residue produced by PEG pyrolysis had effects on their adsorptive and photocatalytic performances of TiO₂-mounted ACCs. It would be a promising technology to integrate adsorption and photocatalysis for TiO₂-mounted ACCs.

© 2008 Elsevier B.V. All rights reserved.

1. Introduction

Adsorption with porous carbon is extensively used for purification of indoor air and water, because these materials possess large specific area and high adsorption capacity [1]. However, there are some disadvantages for adsorption with porous materials, one of which is saturation. In contrast, TiO₂ photocatalyst can decompose various environmental pollutants in gas and liquid phases at room temperature, attracting fairly intensive attention [2]. Recently, some researchers [3–14] reported the combination of TiO₂ photocatalytic activity and adsorption ability of porous carbons. One of the present authors (M.I.) pointed out that there are two kinds of composites [4] between TiO₂ and carbon: carbon-coated TiO₂ and TiO₂-mounted porous carbon. For the former form [5–8], the coated carbon can stabilize the anatase-type structure and prevent the transformation from anatase-type to rutile-type structure as well as endow the catalyst with high adsorptivity. For the latter form [9–14], mounting of TiO₂ onto porous carbon can result in reduction of specific surface area of carbons but offer them extra photocatalytic function. Moreover,

synergistic reaction of combination of carbon with nano TiO₂ can also enhance the photocatalytic performance [10].

Generally activated carbons (ACs) were used for the photocatalyst's support. However, little attention was paid to fibrous carbon adsorbent. In the present work, we selected the cloth type of activated carbon fiber (ACF) and prepared TiO₂-mounted PAN-based activated carbon cloths (ACCs) by a sol–gel method, because this cloth form can easily expose TiO₂-mounted to UV irradiation to improve photocatalytic ability. Their adsorption performance and photocatalytic activity for methylene blue (MB) were investigated. Effect of heat treatment on crystallinity of TiO₂ and pore structure of hybrids, further on their adsorptive and photocatalytic performance was studied.

2. Experimental

The titania sols were prepared by the following method: tetrabutylorthotitanate (reagent grade) and diethanolamine (reagent grade) were dissolved in ethanol, then water and ethanol were mixed together and dropped into the solution when stirring vigorously. Polyethylene glycol (PEG) with average molecular weights of 400 was added to the above solution and subsequently a transparent and light yellow solution was obtained. The TiO₂ was mounted on PAN-based ACC by a dip-coating method. The mixture

* Corresponding author. Fax: +86 10 62771160.

E-mail address: zhhuang@tsinghua.edu.cn (Z.-H. Huang).

Table 1

The preparation details of samples and their pore structure parameters

Sample no.	PEG amount (g/100 mL)	HTT (°C)	S_{BET} (m ² /g)	S_{T} (m ² /g)	S_{Ex} (m ² /g)	v_{Mi} (cm ³ /g)	D_{Av} (nm)	TiO ₂ (%)
P-ACF			1131	1190	35	0.49	0.86	
CT12-N400	0	400	543	557	12	0.24	0.88	23
CT12-N500		500	590	602	20	0.26	0.89	21
CT12-N600		600	664	691	14	0.29	0.87	26
CT12-N700		700	736	730	21	0.33	0.93	27
CT12-N800		800	696	712	38	0.30	0.89	28
CT22-N400	1.5	400	645	631	23	0.29	0.95	27
CT22-N600		600	714	708	23	0.32	0.93	28
CT22-N800		800	771	775	48	0.33	0.91	25
CT32-N400	2.5	400	598	627	19	0.26	0.87	29
CT32-N600		600	644	656	20	0.29	0.9	28
CT32-N800		800	701	738	45	0.30	0.87	28

HTT denotes heat-treatment temperature; S_{BET} , S_{T} , S_{Ex} denote BET, total and external specific surface area, respectively; v_{Mi} denotes micropore volume; D_{Av} denotes average pore size. S_{T} , S_{Ex} and v_{Mi} were calculated by α_s plot; S_{BET} was calculated by BET equation; D_{Av} was calculated by 4 V/S.

was dried at 100 °C and then heat-treated in nitrogen at different temperatures for an hour. The prepared samples were denoted as CTx2-Ny00 (“x = 1, 2, 3” denotes different amount of PEG, “2” denotes coating times, “N” denotes heat treatment in nitrogen, “y00” denotes heat treat temperature from 400 to 900 °C). Pore structure was measured by nitrogen adsorption performed at 77 K (Quantachrome, Autosorb 3). XRD patterns of samples were recorded with scanning speed of 4 °C/min using Cu K α radiation from an 18 kV source (Rigaku, RINT-2000). The morphologies of prepared samples were observed on SEM microscope (AMRAY1820, US). Content of carbon in samples was measured through the combustion of carbon in air at 1000 °C by using TG apparatus (V-560, Japan).

Pieces of sample (1.5 cm \times 1.5 cm) were dispersed into a 2.94×10^{-4} mol/L of methylene blue (MB, reagent grade) solution of 100 mL in a beaker and stirred overnight in the dark. Then the sample saturated with MB in the dark was transferred into 100 mL, 2.94×10^{-5} mol/L of MB solution under UV irradiation (365 nm) from a black light in a box. The decomposition of MB was followed by measuring the absorbance of the solution as a function of UV irradiation time.

3. Results and discussions

3.1. Characterization of TiO₂-mounted ACCs

Table 1 lists the preparation details of samples and changes of pore structure of hybrids. Fig. 1 shows scanning electron

micrographs (SEM) of untreated sample and a representative heat-treated sample of CT12-N800. It was observed that homogeneous thin film could be formed at the surface of ACF by a dip-coating method. When heat-treated in nitrogen at high temperature, however, there were some little “thorns” at the surface of the coatings. They should be TiO₂ produced inevitably. It is seen from Fig. 2 that TiO₂ was amorphous when calcined at 400 °C for an hour in the case of CT12 series. The anatase-type TiO₂ formed when increasing treatment temperature. However, the increase in anatase size was not significant. The formation of rutile-type TiO₂ occurred when the treatment temperature was up to 700 °C. For the sample treated at 800 °C for 1 h, broad diffraction lines indicate the formation of considerable rutile phase. When treatment temperature increased to 900 °C, diffraction lines of rutile phase improved while anatase disappeared completely. There were similar crystallinity changes for CT22 and CT 32 series.

The mounted amount of TiO₂ was determined from the mass loss upon heating to 1000 °C in air using TGA, which was almost constant and can be seen in Table 1. Obviously, mounting of TiO₂ resulted in a marked decrease both in specific surface area and pore volume comparing with the pristine ACC. However, the decrease in surface area and pore volume was recovered gradually with increasing heat-treatment temperature. There was a similar change as reported previously [7]. They supposed the decrease in surface area caused by blocking the pore entrances on the surface of activated carbon by fine particles of TiO₂. The particles of TiO₂ became larger by increasing the heat-treatment temperature,

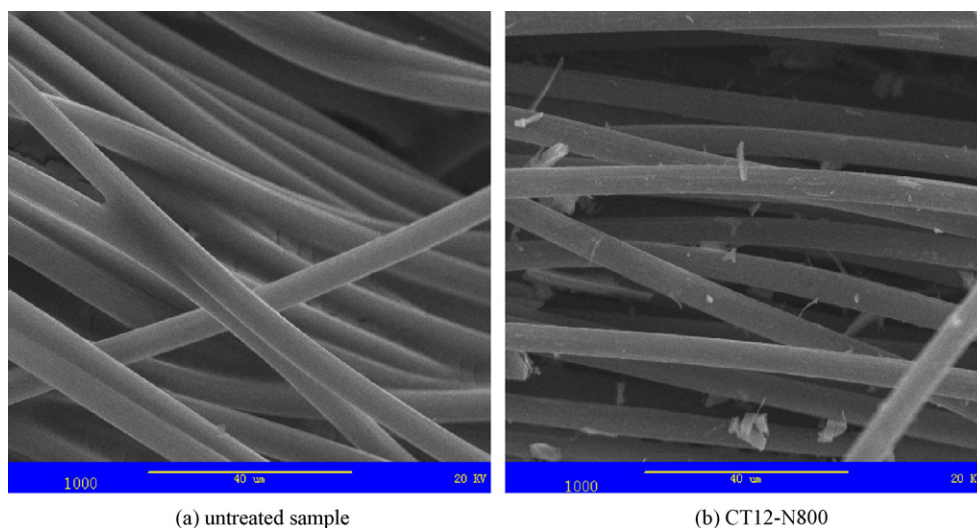


Fig. 1. Scanning electron micrographs of (a) untreated sample and (b) CT12-N800.

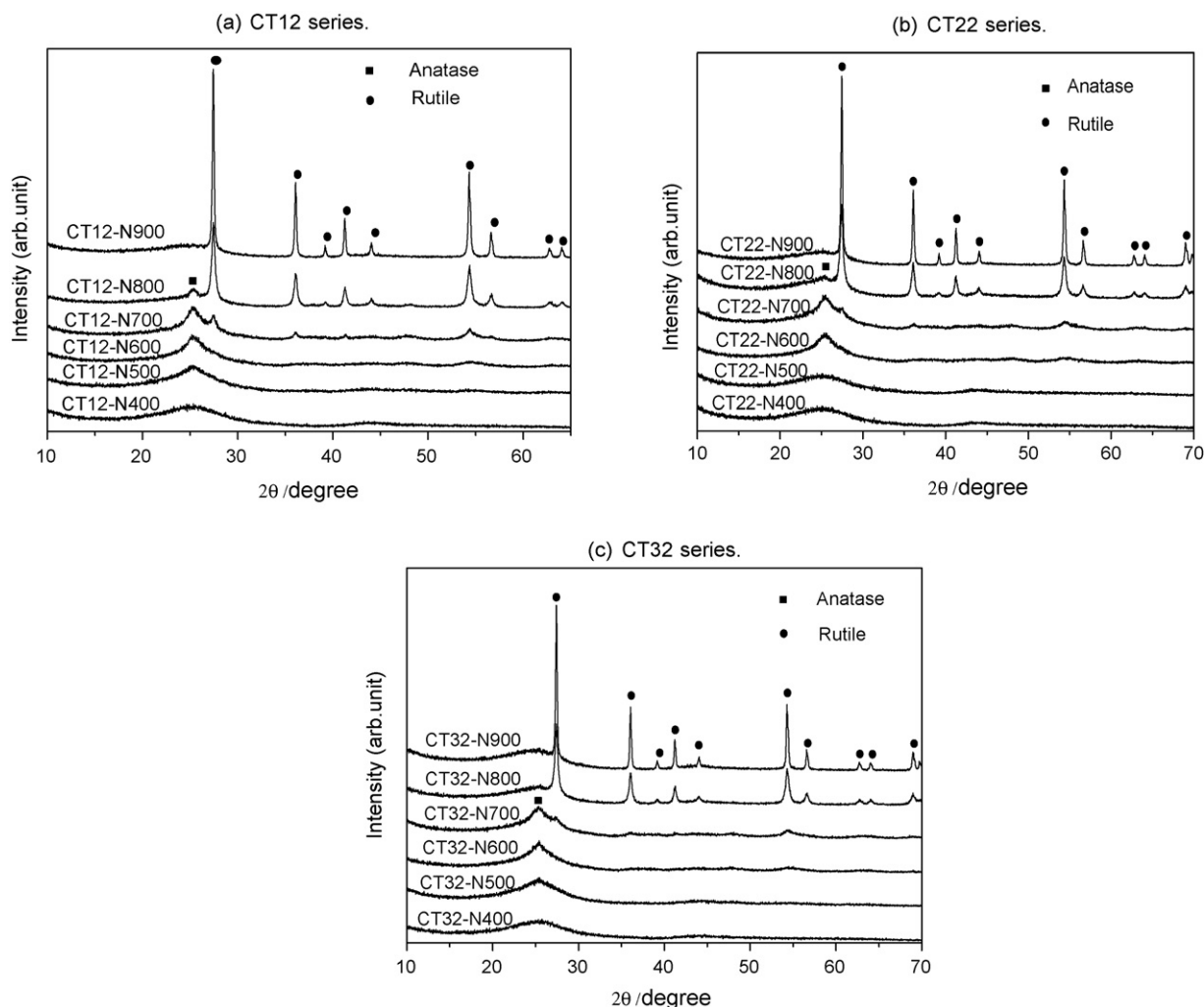


Fig. 2. XRD patterns of (a) CT12 series, (b) CT22 series and (c) CT32 series.

which resulted in making the blocking of pore entrance less efficient. It can be also seen in Table 1 that the BET surface area and pore volume increased for the samples obtained from PEG-added sol at the same treatment temperatures. However, the effect of pore former was weakened when raising its adding amount.

3.2. Adsorption and photocatalytic activities of TiO₂-mounted ACCs

TiO₂-mounted ACC samples were dispersed into a higher concentration of MB solution in the dark overnight for adsorption firstly. The adsorption capacities for MB against treatment temperature were shown in Fig. 3. It is obvious that MB can pass through TiO₂ coating and reach the pores of ACF. All samples exhibited high adsorption capacities due to abundant porosities of ACFs. For three series of samples, different treatment temperatures resulted in different pore structures, leading to different adsorption amounts for MB. The capacities increased with the increasing treatment temperature, corresponding to the changes of pore volume and specific surface area. If we compare CT12 series and CT22 series, we might find that the latter series possessed somewhat lower capacities although higher surface areas and pore volumes. These might be ascribed to different interface characteristics. PEG by pyrolysis produced pores in the TiO₂. During the heat process in nitrogen, a little amount of carbon would be remained and thus coat the surface of TiO₂. It is reported [5–8] that coated carbon can hinder

the growth of the anatase crystal and prevent the transformation to rutile-type. However, due to very little amount of carbon, these effects were less efficient, which can be confirmed in XRD patterns as showed in Fig. 2. Nevertheless, we supposed that the negligible

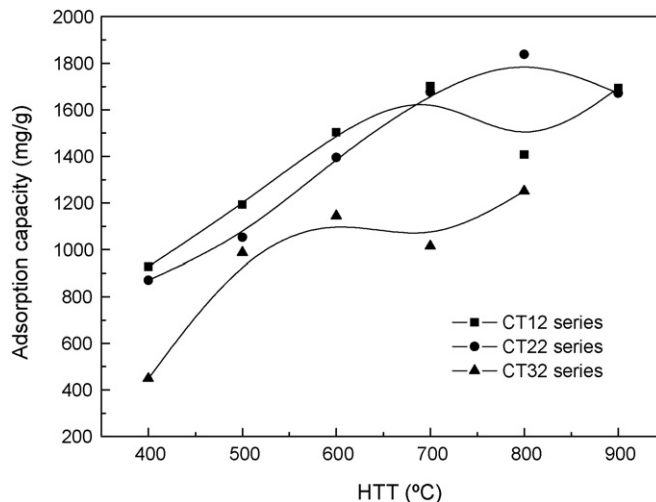


Fig. 3. Adsorption capacity of samples for MB (2.94×10^{-4} mol/L).

carbon influence the interface of TiO_2 and ACF, being detrimental to the adsorption of ACFs. It can be seen from Fig. 3 that CT32 series had lower capacities in comparison with CT22 series because of adding more PEG in TiO_2 precursor.

After adsorption equilibrium was reached in the dark, the sample saturated with MB was transferred into MB solution with a low concentration under UV irradiation for photocatalytic reactions. For three series of samples, Fig. 4 shows the plots of changes

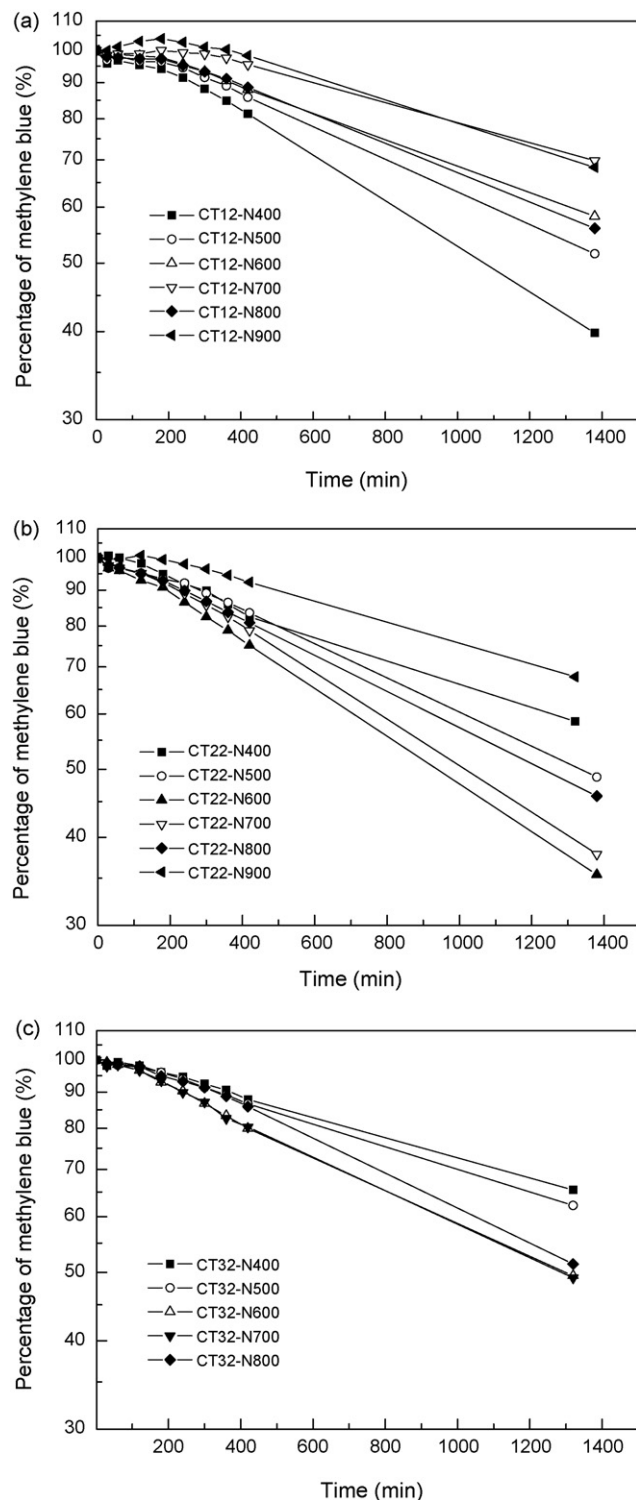


Fig. 4. Changes in MB solution with irradiation time for (a) CT12 series, (b) CT22 series and (c) CT32 series.

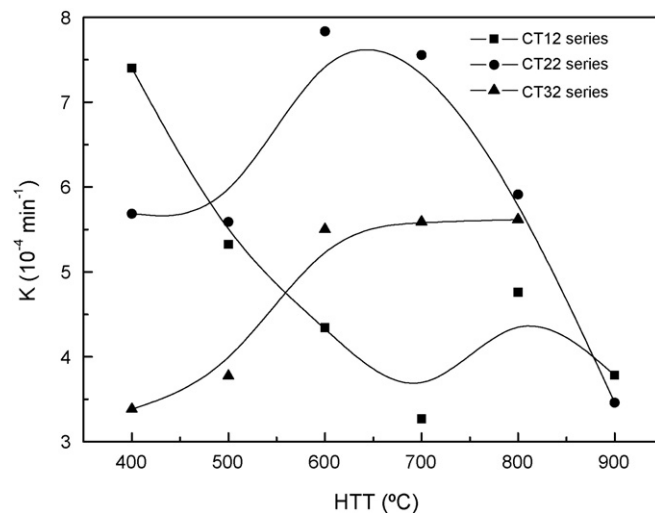


Fig. 5. Rate constants for MB decomposition versus heat-treatment temperatures.

of MB in solution in logarithmic scale against irradiation time of UV rays. In the beginning process, MB concentrations in the solution changed smoothly, even increased for some samples. Subsequently, MB concentrations leveled off then decreased linearly. The beginning processes were supposed to be that TiO_2 -mounted firstly decomposed MB pre-adsorbed in ACF. Moreover, some MB could desorb and enter into solution due to higher adsorption amount and lower decomposition rate. It is obvious that the adsorption capacity might influence the beginning stage of the process. For three series of samples, the higher the adsorption capacity, the more distinct the convex plot in the beginning was.

The rate constants for MB decomposition reaction were shown in Fig. 5, which were determined from linear relation of logarithm of relative concentration of MB. There were quite different changes of rate constants upon treatment temperature although the three series of samples possess similar crystallinities at the same treatment conditions. This might be ascribed to their pore structure and interface characteristics. In the case of CT12 series, the rate constants decreased with treatment temperature. This changing trend went inversely to the plot of CT12 series in Fig. 3. It is surprising that the changes were consistent with the singular point of CT12-N800 in both plots. The more the adsorptive amount, the more the amount to be decomposed was. At that time, the effect of crystallinity was not so significant.

For CT22 and CT32 series, PEG endowed pores and a bit of carbon in TiO_2 by pyrolysis, resulting in different photocatalytic activities. In the case of CT22-N400 and CT32-N400, carbon residues might coat TiO_2 and influence the irradiation, leading to their lower decomposition rate. More PEG produced larger amount of carbon, thus the rate constant of CT32-N400 was lower than CT22-N400's. For the same reason, the plot of CT32 series was at lower position as shown in Fig. 5. However, pores produced in TiO_2 favored diffusion and mass transfer, making the effect of crystallinity emerge. It was reported [15] that the rate constant of TiO_2 for MB decomposition increased up to a maximum at around 700 $^{\circ}\text{C}$ and then decreased with increasing temperature, suggesting a strong dependence of rate constant on crystallinity of anatase phase. There was a similar trend for the TiO_2 only as porous structure mounted on ACCs. The present results showed that the photocatalytic activity of TiO_2 mounted on ACCs depended strongly not only on the content and crystallinity of the anatase phase but also on the pore structure. Therefore, both the adsorption capacity and the photocatalytic activity of porous

TiO₂ mounted on ACC could be improved by annealing at a high temperature. It can be obtained that an optimal sample for the present condition is CT22-N700.

4. Conclusion

In conclusion, photoactive TiO₂ can be homogeneously mounted on PAN-based ACC by a process of dip-coating and subsequent annealing in nitrogen atmosphere. The coating of TiO₂ gel resulted in a remarkable decrease in specific surface area and pore volume comparing with the pristine ACC, which was recovered gradually with increasing heat-treatment temperature. Besides crystallinity of TiO₂ can be modified by treatment condition, its pore structure can be postulated by adding different amount of PEG. Adsorption and degradation of MB on TiO₂-mounted ACCs showed that both pore structure of hybrids and crystallinity of TiO₂ as well as the carbon residue had effects on their adsorptive and photocatalytic performances. For the present condition, an optimal sample was CT22-N700 which synchronously possessed almost the highest adsorption capacity and photocatalytic activity. It suggests that it would be a promising technology to integrate adsorption and photocatalysis with TiO₂-mounted ACCs: in the dark, the adsorption occurs, while under the UV light both adsorption and photocatalysis processes are expected to occur.

Acknowledgements

The authors would like to appreciate the financial support of National High Technology Research and Development Program of China (863 Program) (No. 2007AA061405).

References

- [1] Z.H. Huang, F.Y. Kang, Y.P. Zheng, J.B. Yang, K.M. Liang, Carbon 40 (2002) 1363.
- [2] D.F. Ollis, H. Al-Ekabi (Eds.), Photocatalytic Purification and Treatment of Water and Air, Elsevier, Amsterdam, 1993.
- [3] Z.H. Huang, D.P. Xu, F.Y. Kang, J.M. Hao, New Carbon Mater. 19 (2004) 229.
- [4] T. Tsumura, N. Kojitani, H. Umemura, M. Toyoda, M. Inagaki, Appl. Surf. Sci. 196 (2002) 429.
- [5] T. Tsumura, N. Kojitani, I. Izumi, N. Iwashita, M. Toyoda, M. Inagaki, J. Mater. Chem. 12 (2002) 1391.
- [6] B. Tryba, T. Tsumura, M. Janus, A.W. Morawski, M. Inagaki, Appl. Catal. B 50 (2004) 177.
- [7] M. Inagaki, Y. Hirose, T. Matsunag, T. Tsumur, M. Toyoda, Carbon 41 (2003) 2619.
- [8] L. Zhang, P. Liu, Z. Su, J. Mol. Catal. A 248 (2006) 189.
- [9] H. Uchida, S. Itoh, H. Yoneyama, Chem. Lett. (1993) 1995.
- [10] H. Yoneyama, T. Torimoto, Catal. Today 58 (2000) 133.
- [11] M. Toyoda, Y. Nanbu, T. Kitob, M. Himno, M. Inagaki, Desalination 159 (2003) 273.
- [12] B. Tryba, A.W. Morawski, M. Inagaki, Appl. Catal. B 41 (2003) 427.
- [13] B. Tryba, A.W. Morawski, M. Inagaki, Appl. Catal. B 46 (2003) 203.
- [14] D.P. Xu, Z.H. Huang, F.Y. Kang, et al. J. Wuhan Univ. Tech. Mater. Sci. Ed. 22 (2007) 450.
- [15] M. Inagaki, R. Nonaka, B. Tryba, A.W. Morawski, Chemosphere 64 (2006) 437.